論文の内容の要旨

Discovery and Application of Size-Selective Rim Binding Modes of Cyclodextrins

（シクロデキストリン口縁部によるサイズ選択的結合能の発見とその応用）

花山　博紀

1. Introduction

α, β, and *γ*-Cyclodextrins (CDs) resemble a doughnut bearing a cavity, a narrower rim, and a wider rim (Figure 1a), and are produced on a 10,000-ton scale worldwide for food, pharmaceutical, and other applications.[1] A variety of industrial applications have been developed because of their unique properties such as solubilization and stabilization of molecules and particles, ascribed almost exclusively to cavity binding (CB) to the guest. On the other hand, narrow and wide rim binding (nRB and wRB) has seldom been discussed[2] due to the difficulty in the detection of RB in a mobile equilibrium in the solution, even though there are some cases of solubilization of molecules larger than cavity size of CDs. To investigate the rim binding of CDs, we focused on the binding of CDs to a library of size-different hydrophobic hemispherical apexes of carbon nanohorns (NHs) ranged between 4 Å to 10 Å in radius (Figure 1b,c) to bring the complexes out of equilibrated solution. Statistical analysis of single CD molecules by transmission electron microscopy (TEM) and bulk NMR analysis ($[CD_f]$) were combined to obtain the binding constants at variable temperature (Figure 1d), and the thermodynamic parameters were obtained to clarify the mechanism. As shown in Figure 1d and e, the ratio of concentration of CD-free and CD-bound NHs ($[xNH_f]/[xNH_b]$) was calculated as a ratio of the observed numbers of CD-free and CD-bound NHs ($\#(xNH_f)/\#(xNH_b)$) in TEM, was used to calculate the binding constants.

In this thesis study, I carried out both structural identification and thermodynamic analysis of RB by using electron microscopy, and revealed the similarity of RB to CB in thermodynamics, which suggests non-negligible role of RB in CD binding. Then, I demonstrated the solubilization of a large hydrophobic material with CDs due to shape-cognitive adsorption to apexes of NHs, and as a result, the purification of NH aggregate was achieved via rim binding of CDs.

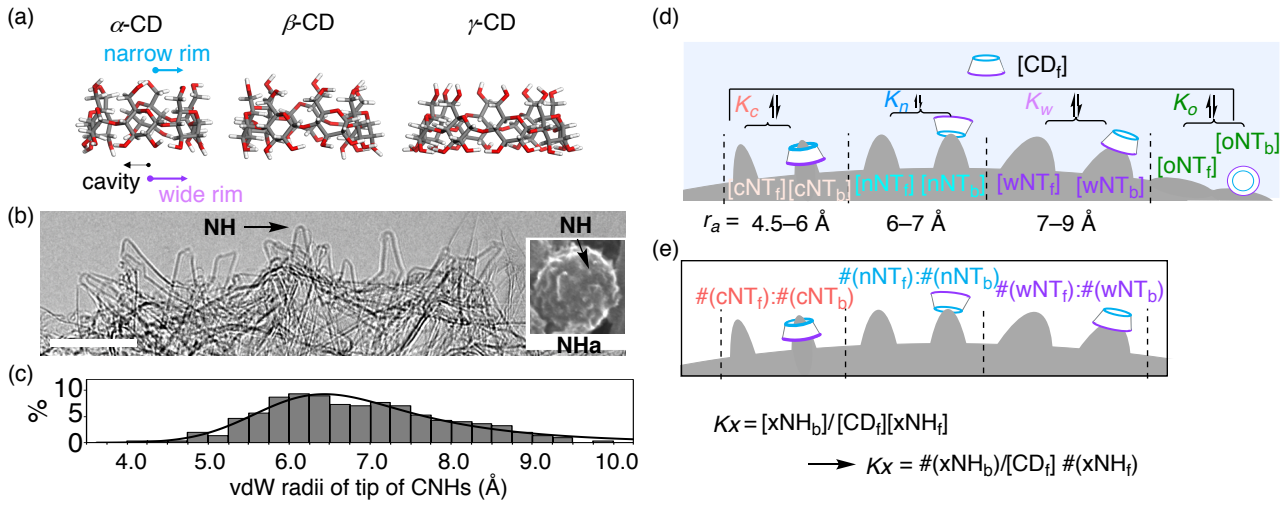

Figure 1. The characteristic of cyclodextrins and carbon nanohorn (a) Molecular structure of α-, β- and γ-CDs, (b) NHs on the surface of NH aggregates (scale bar: 5 nm; inset: SEM image of NH aggregate), (c) Size distribution of tips of NHs. Black line shows ex-gaussian fitting curve. (d) Schematic image of the binding of g-CD on a NH library. γ-CD binds NTs of apex radius (r_a) between 4.5 Å and 9 Å with partial equilibrium constants K_x (x = c, n, w, o). Concentration of free CD in water as [CD_f], and those of CD-bound (b) and CD-free (f) NH in binding mode x as [xNH_b] or [xNH_f]. (e) The numbers of xNH_b and xNH_f were counted using SMART-EM.

2. Electron microscopic and thermodynamic analysis of rim-binding of CDs on the tip of NHs

Electron microscopic investigation of the CD binding mode on the surface of NH revealed a significant contribution of RB to the surface binding. CD/NH aggregates were quickly separated from the equilibrated aqueous solution at 298 K (25 °C), 308 K (35 °C), 323 K (50 °C), 343 K (70 °C) for electron microscopic and thermodynamic analysis. TEM images of binding structure of CDs on NHs showed the existence of RB, where CD bound on the tips larger than the cavity size of γ-CD as shown in Fig. 2b, c. On the other hand, Fig. 2a showed the cavity binding (CB) of γ-CD.

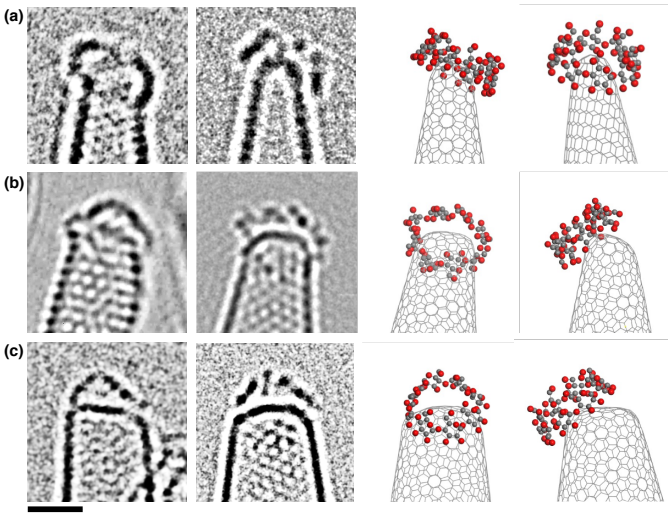

Figure 2. Representative TEM image and simulation of γ-CD/NH γ-CD on the tip of NH in (a) CB mode, (b) nRB mode and (c) wRB mode. (left: TEM image, middle: simulation image, right: molecular model from front and another angle; scale bar: 1 nm).

The statistical analyses over thousands of NHs showed that α- and β-CD had mainly one peak and γ-CD had three peaks (Figure 3a) in the histograms of the ratio of CD-bound NH per total number of NHs. Considering TEM image (Fig 2a) and the sizes of cavity and two rims (orange, blue, and purple bars at the top of histograms), α- and β-CDs showed a large nRB (blue) and small wRB (purple) and γ-CD had CB (orange) below vdW radius of 6 Å in addition to small nRB (blue) and large wRB.

The obtained statistical data was used for the calculation of equilibrium constants of each binding modes (K_c, K_n, K_w, Figure 1e) combined with the concentration of free CDs in water separately determined from NMR measurements of filtrate of the dispersion. The van't Hoff plot from binding constants at four different

temperature (Figure 3b) revealed thermodynamic properties of CB and RBs of each CDs (Table 1). We can see that the nRB and wRB of α- and β-CD are controlled by entropy. On the other hand, nRB and wRB of γ-CD were more enthalpically favored and lost some extent of entropic gain. We considered that more flexible structure of γ-CD than that of α- and β-CD helped γ-CD to find the better conformation to maximize the enthalpic gain while losing entropy more than α- and β-CDs. As a result, CB and RB modes of γ-CD are indistinguishable in terms of thermodynamic features due to similar enthalpy and entropy gain.

Table 1. Binding constants and thermodynamic parameters of CB and RB for α-, β- and γ-CD at 298 K.

		K_x (M^{-1})	ΔG (kJ/mol)	ΔH (kJ/mol)	ΔS (J/(mol•K))	$-T\Delta S$ (kJ/mol)
α-CD	nRB	$3.4 \pm 0.7 \times 10^5$	−31.4 ± 2.6	−5.7 ± 1.9	86 ± 6	−25.7 ± 1.8
	wRB	$4.0 \pm 0.9 \times 10^4$	−26.4 ± 6.0	0.2 ± 4.4	88 ± 14	−26.3 ± 4.1
β-CD	nRB	$1.2 \pm 0.2 \times 10^6$	−34.6 ± 1.9	−2.7 ± 1.4	107 ± 4	−31.9 ± 1.3
	wRB	$5.6 \pm 1.4 \times 10^5$	−32.7 ± 2.5	−2.0 ± 1.8	103 ± 6	−30.6 ± 2.2
γ-CD	CB	$9.5 \pm 2.7 \times 10^5$	−34.0 ± 1.4	−19.0 ± 1.0	50 ± 3	−15.0 ± 1.0
	nRB	$2.9 \pm 1.0 \times 10^5$	−31.3 ± 2.4	−13.8 ± 1.7	59 ± 5	−17.5 ± 1.6
	wRB	$5.2 \pm 1.5 \times 10^5$	−32.5 ± 2.8	−15.6 ± 2.0	57 ± 6	−16.9 ± 1.9

Figure 3c visually showed the comparison of obtained thermodynamic parameters in CD/NH (markers) and previously reported 500+ thermodynamic parameters obtained by calorimetry (black dots). We found similar slope for the binding data obtained in the present study (colored markers), while y-intercept is smaller by 19.1 kJ/mol as expected from the higher hydrophobicity of the NH surface than molecules previously investigated. Importantly, the thermodynamic data of the CB and RB modes for γ-CD (orange box) in Table 4 are almost indistinguishable, compared with the wide distribution of thermodynamic data in CD bindings as shown in Figure 3c, without simultaneous investigation of binding structure of CDs. This similarity of the data suggests that RB plays non-negligible roles in the molecular recognition previously ascribed solely to CB and the cavity inclusion chemistry of CDs represents only a fraction of a much broader spectrum of guest recognition.

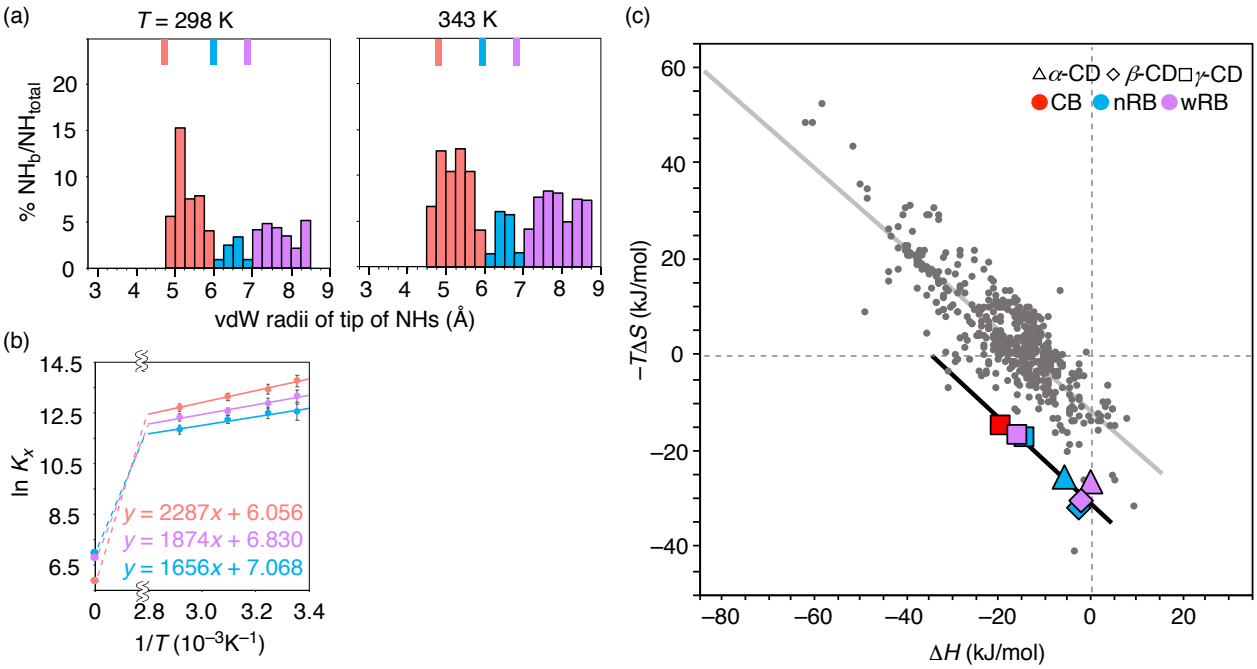

Figure 3. Statistical and thermodynamic analysis of binding of CD on tips of NHs (a) histograms of the ratio of γ-CD–bound NH per the total number of NHs examined. The sum in each binding mode was written in the right side (top: CB, middle: nRB, bottom: wRB). (b) van't Hoff plot of CB (top) and RB (nRB: bottom, wRB: middle) of γ-CD/NH. (c) ΔH-TΔS plot of thermodynamics of reported CD/molecule complexes (black dots), CD/NH (triangle: α-CD/NH, diamond: β-CD/NH, square: γ-CD/NH, CB: red, nRB: blue, wRB: purple).

3. Solubilization and purification of CNH aggregates by using cyclodextrins as shape-cognitive surfactants

I found that only 1 wt% of α-, β- and γ-CD solubilized NH aggregates efficiently via CB and RB to the tip and extracted pure NH aggregates from a commercially available sample with 10 wt% of graphitic ball-shaped impurity (GB), while linear analogue (glucose, amylose) did not solubilize NH aggregates in the same conditon. I established the procedure to allow for gram-scale purification of NH aggregates as shown in Figure 4a. α-CD was used in the purification because it was more easily detached from the surface of NH aggregates than γ-CD by washing with water. Thus, 2.00 g of CNH aggregates were dispersed with 1 wt% of α-CD in 800 mL of water after sonication for 5 min. Then, after following centrifugation at 1500*g* for 10 min, top 80% of the dispersion was filtrated and the filter cake were washed with water and ethanol to give 1.44 g of purified NH aggregates (72%). Thermogravimetric (TG) analysis confirmed that GB, which burned around 800 °C (Figure 4b, black line), was successfully removed in a large-scale purification (Figure 4b, gray line). Importantly, the TG curve was distinctively different from that of NH aggregate purified non-selectively by just centrifuged in ethanol dispersion without CDs, where a fraction of high burning point around 700 °C was enriched (Figure 4b, dotted line). This result suggested the purification with CDs were based on the shape-recognition and not solely on the density of materials. The purification protocol of the NH aggregates enabled us to prepare GB-free amino-NH aggregates,[3] which serves as a for specimen support for single molecular atomic-resolution real time electron microscopy (SMART-EM) studies.[4] These results showed that the solubilization of hydrophobic material was achieved only by RB modes.

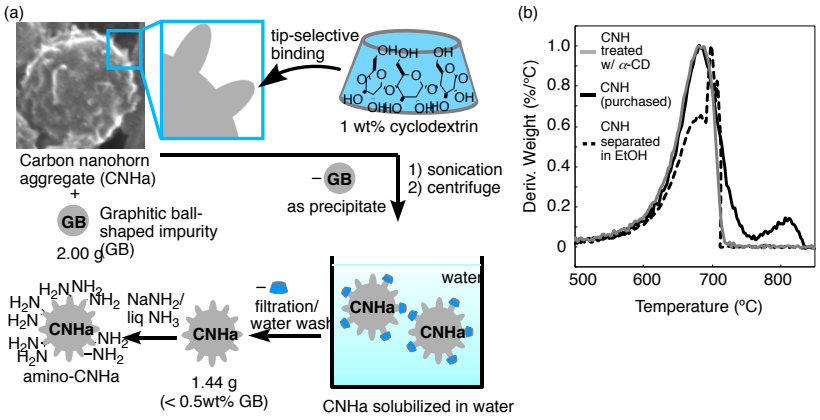

Figure 4. Solubilization and purification of CNH aggregates by CDs. (a) Gram-scale purification of CNH aggregates by tip binding of CDs in water followed by centrifugation and filtration, and amination. (b) Temperature derivatives of TG curves of CNH aggregates separated with α-CD (gray), as-purchased CNH aggregate (black) and CNH aggregates in supernatant of EtOH dispersion after centrifugation (dotted).

4. Conclusion

In summary, we found the CDs recognized far broader range of hydrophobic entities than so far considered, by utilizing the cavity and the rims. Combination of single molecular study using TEM imaging and bulk experiments enabled us to obtain structural and thermodynamic data spontaneously, and revealed that rim bindings took place with remarkably similar thermodynamics to CB. We expected that the discovery of the rim binding mode urges reinterpretation of the accepted wisdom and foster new ideas of the design of CDs to bind materials out of limitation of cavity sizes efficiently.

5. References

[1] Szejtli, J. *Chem. Rev.* **1998**, *98*, 1743–1754.

[2] de Jesus, M. B. et al, *J. Pharm. Pharmacol.* **2012**, *64*, 832–842.

[3] H. Isobe, et al. *Angew. Chem. Int. Ed.*, **2006**, *45*, 6676.

[4] Nakamura, E. *Acc. Chem. Res.* **2017**, *50*, 1281.